Article:

Bergen, K.J., Shaw, J.H., Leon, L.A. et al. (8 more authors) (2017) Accelerating slip rates on the Puente Hills blind thrust fault system beneath metropolitan Los Angeles, California, USA. Geology, 45 (3). pp. 227-230. ISSN 1943-2682

https://doi.org/10.1130/G38520.1

Accelerating slip rates on the Puente Hills Blind-thrust Fault System beneath metropolitan Los Angeles, California

Kristian J. Bergen[1*], John H. Shaw[1], Lorraine A. Leon[2,3], James F. Dolan[2], Thomas L. Pratt[4], Daniel J. Ponti[5], Eric Morrow[1], Wendy Barrera[6], Edward J. Rhodes[6,7], Madhav K. Murari[8], and Lewis A. Owen[8]

[1]*Department of Earth and Planetary Sciences, Harvard University, Cambridge, Massachusetts, USA*

[2]*Department of Earth Sciences, University of Southern California, Los Angeles, California, USA*

[3] *now at Chevron North America Exploration and Production, Bakersfield, California, USA*

[4]*U.S. Geological Survey, Reston, Virginia, USA*

[5]*U.S. Geological Survey, Menlo Park, California, USA*

[6]*Earth, Planetary and Space Sciences, University of California Los Angeles, Los Angeles, California, USA*

[7]*Department of Geography, University of Sheffield, Sheffield, S10 2TN, UK*

[8]*Department of Geology, University of Cincinnati, Cincinnati, Ohio, USA*

*E-mail: kbergen@fas.harvard.edu

Authors' version of accepted manuscript published in Geology, 2017

ABSTRACT

Slip rates represent the average displacement across a fault over time and are essential to estimating earthquake recurrence for probabilistic seismic hazard assessments. We demonstrate that the slip rate on the western segment of the Puente Hills blind-thrust fault system, which lies directly beneath downtown Los Angeles, California, has accelerated from ≈0.22 mm/yr in the late Pleistocene to ≈1.33 mm/yr in the Holocene. Our analysis is based on syntectonic strata derived from the Los Angeles River, which has continuously buried a fold scarp above the tip of the blind thrust. Significant slip on the fault beneath our field site began during late-mid Pleistocene time and progressively increased into the Holocene. This increase in rate implies that the magnitudes and/or the frequency of earthquakes on this fault segment have increased over time. This challenges the characteristic earthquake model and presents an evolving and potentially increasing seismic hazard to metropolitan Los Angeles.

INTRODUCTION

The Puente Hills blind-thrust fault system (PHT) extends for 40 km across the Los Angeles (LA) basin and presents one of the largest deterministic seismic risks in the United States (Shaw and Shearer, 1999; Dolan et al., 2003; Field et al., 2005) (Fig. 1a). Blind-thrusts do not reach the earth's surface, complicating assessment of their activity and slip rate. Their surface expression, if any exists, is often as fold scarps (e.g., Stein and Yeats, 1989; Shaw and Suppe, 1996; Shaw and Shearer, 1999; Champion et al., 2001). The M_w 6.7 Northridge earthquake dramatically demonstrated the damaging effects of blind-thrust earthquakes, causing 60 fatalities and an estimated $13-$40 billion in damage to the LA region (NOAA NCEI, 1994). The PHT presents an even greater potential hazard due to its size and proximity to the most densely populated regions of LA (Field et al., 2005).

The motivation of our research is to determine a contemporary slip rate on the LA segment of the PHT, which underlies downtown LA. Our site also provides the opportunity to investigate the continuity of slip rates over the past half-million years, thanks to the continual burial of fold scarps by sediment from the LA River. In contrast, most geologic assessments of slip rates rely on paleoseismic methods that sample only the last few tens of thousands of years (e.g., Dolan et al., 2003), or geologic cross sections that define slip rates over millions of years (e.g., Huftile and Yeats, 1995). The intervening several hundred thousand year time span is rarely constrained. Yet, this period has important implications for long-standing questions about the characteristic earthquake model (e.g., Jacoby et al., 1988; Kagan et al., 2012) and temporal earthquake clustering (e.g., Grant and Sieh, 1994; Dolan et al., 2007), as changes in slip rate over time imply changes in earthquake magnitudes, frequency, and/or slip distributions. The implications for probabilistic seismic hazard assessments (PSHA) are perhaps greater, as changes in slip rate would complicate estimates of earthquake recurrence (Youngs and Coppersmith, 1985).

GEOLOGICAL AND SEISMOLOGICAL SETTING

The PHT sits within the LA basin, which contains a thick succession of Quaternary through Cretaceous sedimentary units above Mesozoic basement (Wright, 1991). The PHT was identified as the source of the 1987 M_w 6.0 Whittier Narrows earthquake (Shaw and Shearer, 1999) and includes three main segments: the Coyote Hills, Santa Fe Springs, and LA (Fig. 1). The tips of these faults are overlain by a series

DOI:10.1130/G38520.1

of en echelon anticlines running east-west from Beverly Hills to Orange County (Shaw et al., 2002; Leon et al., 2007). Using earthquake magnitude-scaling relationships for thrust faults (Wells and Coppersmith, 1994), Shaw and Shearer (1999) estimated that the PHT could generate a M_w 7.1 earthquake if the segments ruptured simultaneously and M_w 6.5 – 6.6 if they ruptured independently; consideration of slip/event data, however, suggests potentially larger magnitudes of M_w 7.2–7.5 for multi-segment ruptures (Dolan et al., 2003).

The southern margin of the anticlines above the PHT have narrow forelimbs that are pinned at depth to the upper tiplines of the blind fault ramps (Pratt et al., 2002; Shaw et al., 2002). Pliocene and younger strata thin across the folds, indicating that these units represent growth (syntectonic) stratigraphy (Suppe et al., 1992; Shaw and Suppe, 1994). These growth strata are flood deposits from the LA and San Gabriel Rivers that continually buried the fold scarps, recording the amount of relative uplift as the difference in stratigraphic thickness between the uplifted fold crest and the adjacent footwall trough. Based on these differences, average slip rates over the past 1.6 Ma have been estimated to be 0.44 – 1.7mm/yr across all three segments (Shaw et al., 2002). Subsequent work refined the Holocene slip rate on the Santa Fe Springs segment to ≤0.9 – 1.6 mm/yr (Dolan et al., 2003; Leon et al., 2007).

DATA AND METHODS

We estimate slip rates on the LA segment using seismic-reflection data and a range of dating methods. Industry seismic reflection data image a fold limb with growth stratigraphy above the LA segment (Fig. 1d). High-frequency seismic reflection data (Fig. 1c), a series of continuously cored hollow-stem auger boreholes (Fig. 1b), and a deeper (175 m) mud-rotary borehole (Fig. 1b, 1c) were acquired for this study to constrain the shallow geometry of the fold and determine the most recent fault activity. To provide Pleistocene stratigraphic markers, sequence boundaries from the Ponti et al. (2007) Long Beach area framework were mapped to our high frequency seismic reflection profiles (20-25 km away) using additional well logs and our industry seismic reflection data. Lithological correlations from the boreholes were used to map the fold geometry into the Holocene. Age constraints were provided by marine oxygen isotope stages (MIS) for the sequence boundaries (Ponti et al., 2007; McDougall et al., 2012). For the borehole lithological correlations we used radiocarbon (^{14}C) and single-grain K-feldspar post-IR IRSL (Infra-Red Stimulated Luminescence) dating (Rhodes, 2015; results and technical details in the Supplemental Materials). The fold geometry is consistent with growth stratigraphy deposited above the forelimb of a fault-bend fold (Suppe et al., 1992; Shaw and Shearer, 1999; Pratt et al., 2002) (Fig. 1c and Supplemental Fig. DR1); we used this insight to model the underlying fault geometry and relate uplift to fault slip as described in the Supplemental Materials.

We adopt a probabilistic approach that accounts for uncertainties in both ages and stratigraphic geometries to estimate slip rate probability density functions over a series of time intervals. We developed an autoregressive statistical model (AR) of interval velocities from the nearby La Tijera industry well (Fig. 1a, 1d) to simulate velocity models for depth conversion of our high frequency seismic reflection data. To account for resolution uncertainties, we randomly repositioned the interpreted sequence boundaries within estimated $\pm½\lambda$ (wavelength) resolution limits of the seismic data (Vail et al., 1977). To account for any thickness changes due to differential compaction across the fold, we used exponential porosity-depth relations (Athy, 1930) to estimate depositional thicknesses. Bed dip and sediment thickness changes across the fold were then calculated for each simulation and used to determine fault geometry and slip. Finally, probability distributions for our age determinations were sampled at random and combined with our slip estimates to calculate slip rate probability distributions.

Figure 2 shows the estimated distributions for fold crest depth, trough depth, and structural relief along with associated age distributions. Slip rate distributions are shown in Figure 3 and Supplemental Table DR1d. These are geometrically related to the vertical relief in Figure 2 by corresponding fault dips, shown in Figure 1d and Supplemental Table DR1e. Sedimentation rates based on trough position and age (dark blue in Fig. 2) are shown in Supplemental Figure DR9 and Supplemental Table DR1a. Horizontal shortening and uplift rate distributions are shown in Supplemental Figure DR10 and Supplemental Table 1d.

DISCUSSION

The most recent time period defined by our study is from the top clay horizon (11.7 – 17.6 ka) to the present. The total slip over this period ranges from 17.75 – 22.72 m (2.5 – 97.5 percentile ranges), confirming the occurrence of multiple earthquakes to support our slip rate estimate in this period of 1.13 – 1.73 mm/yr (2.5 – 97.5 percentile ranges). This range is consistent with Holocene slip rates of ≤0.9 – 1.6 mm/yr obtained on the central Santa Fe Springs segment of the PHT (Dolan et al., 2003; Leon et al., 2007), supporting the view that these two segments behave as a linked system and may rupture together in large, M_w ≥7 earthquakes. Comparison of horizontal shortening rates from the top clay to the present of 1.06 - 1.63 mm/yr (2.5 – 97.5 percentile range;

Supplemental Table DR1d) to geodetically determined shortening estimates across the LA region of 4.4 ± 0.8 mm/yr from Bawden et al. (2001) and 4.5 ± 1 mm/yr from Argus et al. (2005), suggests that the LA segment may account for about one half of the modern shortening across the basin.

Examining the slip rate data from earlier time intervals, significant motion on the LA segment at our site began between creation of the Bent Spring and the Harbor sequence boundaries during late-mid Pleistocene time and progressively increased through the late Quaternary (Fig. 3). This is demonstrated in the slip-rate similarity plots in Figure 3, which show the probability that slip rate remains constant across previous time intervals, given the uncertainties in our data. We assessed if slip rates were similar by calculating the difference between them across all time intervals for each individual model iteration, in a stepwise fashion from the present backward in time. Only values meeting the similarity criterion (i.e., could have similar slip rates between time steps) in more recent time intervals were considered for similarity in subsequent steps. To present day, roughly 36% of our simulations had slip rates within 0.25 mm/yr of each other over the two time intervals following creation of the Harbor sequence boundary. Of these, however, none met the 0.25 mm/yr criterion across prior intervals. Increasing the similarity window to 0.5 mm/yr, 9% of our simulations survived to the Bent Spring sequence boundary, and 4 out of 50,000 simulations (8×10^{-5}) satisfied these conditions back to creation of the Upper Wilmington sequence boundary. This demonstrates that the slip rate on the LA segment has almost certainly accelerated since formation of the Bent Spring sequence boundary, and that it likely continued to increase after formation of the Harbor sequence boundary to the present day. This accelerating pattern highlights the importance of using slip rates averaged over recent time periods of most relevance to PSHA. Our results, for example, show that PHT slip rates determined from earlier time intervals and averaged across longer time intervals yield lower estimates of earthquake recurrence than indicated by our most recent slip rates.

We propose three reasons for the observed accelerating slip rate at our site: the frequency of earthquakes could have increased; the average displacement per earthquake could have increased; or both. Given our location at the western margin of the LA segment, we suggest that the most likely explanation is that displacement per earthquake has increased at our study site as the fault tip has propagated laterally to the west. Such behavior has been documented for other blind thrusts (Grothe et al., 2014), and seems plausible here given the location of our site. This implies that the LA segment has grown laterally over the late Quaternary, and may have correspondingly increased its maximum potential earthquake magnitude and seismic hazard. While research on displacement-length relationships for thrust faults is limited, it is generally found that longer fault lengths correspond to greater displacements, supporting our view that lateral fault-tip propagation could increase earthquake magnitude (e.g., Bergen and Shaw, 2010). If this is the case, it directly challenges the characteristic earthquake model assumption of regular, repeating rupture patterns (i.e., rupture size and displacement) on individual fault segments over many earthquake cycles (Grant, 1996). If earthquakes were occurring more frequently instead, or in addition to growing in magnitude, this would imply an increase in loading rates that would also raise seismic hazard on the LA segment of the PHT.

CONCLUSIONS

We establish the evolving slip rate on the western segment of the PHT beneath metropolitan Los Angeles, California, over the last half million years. Prior to 248 ka, the fault exhibited a modest slip rate of ≈0.22 mm/yr. The slip rate accelerated through the late Pleistocene to ≈1.33 mm/yr in the past 17 ka. This significant change in slip rate implies an increasing seismic hazard for the city of Los Angeles. Moreover, it highlights concerns about using slip rates averaged over long geologic time intervals for evolving fault systems in regional seismic hazard assessment.

Our interpretation also has regional implications. As slip rates on the LA segment are increasing, it implies that either slip is being transferred to the PHT from another fault system, the latter of which would have decreasing slip through time (redistributing a constant total hazard to different parts of the basin), or, alternatively, the total shortening rate across the LA basin has increased with time (increasing hazard throughout the basin). In the latter scenario, the PHT could be accommodating all of the increase, or slip rates on multiple fault systems could have increased. These scenarios point to evolution of both the PHT fault system and the regional tectonics, adding complexity to, and likely increasing, the seismic hazard to metropolitan LA.

ACKNOWLEDGMENTS

We offer thanks to the NSF EAR RAPID and Tectonics programs, which facilitated drilling and data collection in a narrow time frame when the site remained accessible (NSF EAR 0946261, EAR 0920947, EAR 0711170 and EAR 0711220). We also acknowledge the Southern California Earthquake Center (SCEC) for supporting early studies of the PHT that laid the groundwork for this investigation, and the USGS earthquake hazards program for contributions to this effort. We also thank the numerous field assistants that helped us acquire data for this study, and Dr. Carling Hay and Dr. Erik Chan for their helpful discussions. We are also indebted to the reviewers (Karl Mueller, Christopher Jackson, Christopher Sorlien, and Kate Scharer) for their helpful comments. Any use of trade, firm, or product names is for descriptive purposes only and does not imply endorsement by the U.S. Government.

REFERENCES CITED

Athy, L.F., 1930, Density, Porosity, and Compaction of Sedimentary Rocks: The American Association of Petroleum Geologists Bulletin, v. 14, p. 1–24.

Argus, D.F., Heflin, M.B., Peltzer, G., Webb, F.H., and Crampe, F., 2005, Interseismic strain accumulation and anthropogenic motion in metropolitan Los Angeles: Journal of Geophysical Research, v. 101, B04401, p. 2156–2202, doi:10.1029/2003JB002934.

Bawden, G., Thatcher, W., Stein, R.S., Hudnut, K., and Peltzer, G., 2001, Tectonic contraction across Los Angeles after removal of groundwater pumping effects: Nature, v. 412, p. 812–815, doi:10.1038/35090558.

Bergen, K.J., and Shaw, J.H., 2010, Displacement profiles and displacement-length scaling relationships of thrust faults constrained by seismic-reflection data: Geological Society of America Bulletin, v. 122, p. 1209–1219, doi:10.1130/B26373.1.

Champion, J., Mueller, K., Tate, A., and Guccione, M., 2001, Geometry, numerical models and revised slip rate for the Reelfoot fault and trishear fault-propagation fold, New Madrid seismic zone, Engineering Geology, v. 62 p. 31-49.

Dolan, J.F., Bowman, D.D., and Sammis, C.G., 2007, Long-range and long-term fault interactions in Southern California: Geology, v. 35, p. 855–858, doi:10.1130/G23789A.1.

Dolan, J.F., Christofferson, S.A., and Shaw, J.H., 2003, Recognition of paleoearthquakes on the Puente Hills blind thrust fault, California: Science, v. 300, p. 115–118, doi:10.1126/science.1080593.

Field, E.H., Seligson, H.A., Gupta, N., Gupta, V., Jordan, T.H., and Campbell, K.W., 2005, Loss Estimates for a Puente Hills Blind-Thrust Earthquake in Los Angeles, California: Earthquake Spectra, v. 21, p. 329–338, doi:10.1193/1.1898332.

Grant, L.B., and Sieh, K.E., 1994, Paleoseismic Evidence of Clustered Earthquakes on the San-Andreas Fault in the Carrizo Plain, California: Journal of Geophysical Research, v. 99, p. 6819–6841, doi:10.1029/94JB00125.

Grant, L.B., 1996, Uncharacteristic earthquakes on the San Andreas Fault: Science, v. 272, p. 826–827, doi:10.1126/science.272.5263.826.

Grothe, P.R., N. Cardozo, K. Mueller, and T. Ishiyama, 2014, Propagation history of the Osaka- wan blind thrust, Japan, from trishear modeling, *Journal of Structural Geology,* v. 58, p. 79- 94.

Huftile, G.J., and Yeats, R.S., 1995, Convergence rates across a displacement transfer zone in the Western Transverse Ranges, Ventura basin, California, Journal of Geophysical Research, v. 100, p. 2043-2067.

Jacoby, G.C., Sheppard, P.R., and Sieh, K.E., 1988, Irregular Recurrence of Large Earthquakes Along the San-Andreas Fault — Evidence From Trees: Science, v. 241, p. 196–199, doi:10.1126/science.241.4862.196.

DOI:10.1130/G38520.1

Kagan, Y.Y., Jackson, D.D., and Geller, R.J., 2012, Characteristic Earthquake Model, 1884–2011, RIP: Seismological Research Letters, v. 83, p. 951–953, doi:10.1785/0220120107.

Leon, L. A., Christofferson, S. A., Dolan, J. F., Shaw, J. H., and Pratt, T. L., 2007, Earthquake-by-earthquake fold growth above the Puente Hills blind thrust fault, Los Angeles, California: Implications for fold kinematics and seismic hazard: Journal of Geophysical Research, v. 112, B03S03, p. 2156–2202, doi.10.1029/2006JB004461.

McDougall, K., Hillhouse, J., Powell, C., II, Mahan, S., Wan, E., and Sarna-Wojcicki, A.M., 2012, Paleontology and geochronology of the Long Beach core sites and monitoring wells, Long Beach, California: U.S. Geological Survey Open-File Report 2011–1274, 235 p.

NOAA, NCEI, 1994, Significant Earthquake: California, Northridge: http://www.ngdc.noaa.gov/nndc/struts/results?eq_0=5372&t=101650&s=13&d=22,26,13,12&nd=display (**January, 2014**).

Plesch, A., Shaw, J.H., Benson, C., Bryant, W.A., Carena, S., Cooke, M., Dolan, J.F., Fuis, G., Gath, E., Grant, L., Hauksson, E., Jordan, T.H., Kamerling, M., Legg, M., Lindvall, S., Magistrale, H., Nicholson, C., Niemi, N., Oskin, M.E., Perry, S., Planansky, G., Rockwell, T., Shearer, P., Sorlien, C., Suess, M.P., Suppe, J., Treiman, J., and Yeats, R., 2007, Community fault model (CFM) for southern California: Bulletin of the Seismological Society of America, v. 97, p. 1793–1802, doi:10.1785/0120050211.

Ponti, D.J., Ehman, K.D., Edwards, B.D., Tinsley, J.C., III, Hildenbrand, T., Hillhouse, J.W., Hanson, R.T., McDougall, K., Powell, C.L., II, Wan, E., Land, M., Mahan, S., and Sarna-Wojcicki, A.M., 2007, A 3-Dimensional Model of Water-Bearing Sequences in the Dominguez Gap Region, Long Beach, California: U.S. Geological Survey Open-File Report 2007–1013, 34 p.

Pratt, T.L., Shaw, J.H., Dolan, J.F., Christofferson, S., Williams, R.A., Odum, J.K., and Plesch, A., 2002, Shallow seismic imaging of folds above the Puente Hills blind-thrust fault, Los Angeles, California: Geophysical Research Letters, v. 29, p. 18–1–18–4.

Rhodes, E.J., 2015, Dating sediments using potassium feldspar single-grain IRSL: initial methodological considerations, Quaternary International, v. 362, p. 14-22, http://dx.doi.org/10.1016/j.quaint.2014.12.012.

Shaw, J. and J. Suppe, 1994, Active faulting and growth folding in the eastern Santa Barbara Channel, California, *Geological Society of America Bulletin*, v. 106/5, p. 607-626.

Shaw, J.H., and Suppe, J., 1996, Earthquake hazards of active blind-thrust faults under the central Los Angeles basin, California: Journal of Geophysical Research, v. 101, p. 8623–8642, doi:10.1029/95JB03453.

Shaw, J.H., and Shearer, P.M., 1999, An elusive blind-thrust fault beneath metropolitan Los Angeles: Science, v. 283, p. 1516–1518, doi:10.1126/science.283.5407.1516.

Shaw, J.H., Plesch, A., Dolan, J.F., Pratt, T.L., and Fiore, P., 2002, Puente Hills blind-thrust system, Los Angeles, California: Bulletin of the Seismological Society of America, v. 92, p. 2946–2960, doi:10.1785/0120010291.

Shaw, J.H., Plesch, A., Tape, C., Suess, M.P., Jordan, T.H., Ely, G., Hauksson, E., Tromp, J., Tanimoto, T., Graves, R., Olsen, K., Nicholson, C., Maechling, P.J., Rivero, C., Lovely, P., Brankman, C.M., and Munster, J., 2015, Unified Structural

Representation of the southern California crust and upper mantle: Earth and Planetary Science Letters, v. 415, p. 1–15, doi:10.1016/j.epsl.2015.01.016.

Stein, R.S., and Yeats, R.S., 1989, Hidden Earthquakes: Scientific American, v. 260, p. 48–57, doi:10.1038/scientificamerican0689-48.

Suppe, J., Chou, G., and Hook, S., 1992, Rates of folding and faulting determined from growth strata, *in* McClay, K., ed., Thrust tectonics: London, Chapman Hall, p. 105–121, doi:10.1007/978-94-011-3066-0_9.

Vail, P.R., Todd, R.G., and Sangree, J.B., 1977, Seismic stratigraphy and global changes of sea level: Part 5. Chronostratigraphic significance of seismic reflections: Section 2. Application of seismic reflection configuration to stratigraphic interpretation, *in* Payton, C.E., ed., Seismic Stratigraphy - Applications to Hydrocarbon Exploration: American Association of Petroleum Geologists Memoir 26, p. 99–116.

Wells, D.L., and Coppersmith, K.J., 1994, New Empirical Relationships Among Magnitude, Rupture Length, Rupture Width, Rupture Area, and Surface Displacement: Bulletin of the Seismological Society of America, v. 84, p. 974–1002.

Wright, T.L., 1991, Structural Geology and Tectonic Evolution of the Los Angeles Basin, California, *in* Biddle, K., ed., Active Margin Basins: American Association of Petroleum Geologists Memoir 52, p. 35–134.

Youngs, R.R., and Coppersmith, K.J., 1985, Implications of Fault Slip Rates and Earthquake Recurrence Models to Probabilistic Seismic Hazard Estimates: Bulletin of the Seismological Society of America, v. 75, p. 939–964.

FIGURE CAPTIONS

Figure 1a. Perspective view of the PHT from the Southern California Earthquake Center (SCEC) Community Fault Model (Plesch et al., 2007), highlighting the LA segment in red. The locations of the seismic reflection profiles B-B' and C-C' in Figures 1c and 1d are marked in Figure 1a: the borehole profile A-A' is within B-B'. Surface topography is 5:1 vertically exaggerated; other dimensions are 1:1. b. Shallow borehole profile. Boreholes 1–10 are continuously cored hollow-stem auger boreholes. Borehole D1 was drilled with both hollow-stem auger and mud-rotary techniques to sample a greater depth range. To produce the vertical relief observed across the clay and silt unit (green) given the estimated fault dips (see Fig. 1d), a total of 17.75 – 22.72 m slip is required (2.5 – 97.5 percentile ranges). This indicates the occurrence of several earthquakes between deposition of the clay and silt layer and the overlying organic-rich black clay that buttresses the fold. The geometry of the top clay and ^{14}C ages from wells 8 and 5 were used for our most recent slip rate estimates. c. Weight drop seismic reflection profile, depth-converted using the SCEC Community Velocity Model with geotechnical layer (CVMH) (Shaw et al., 2015). d. Industry seismic reflection profile showing the broader LA segment fold structure. The apparent fault dip range in red encompasses the 2.5 – 97.5 percentile range from our simulations as shown in the adjacent histogram.

Figure 2. Thickness and vertical relief change over time. Normalized probability distributions of crest, trough, and vertical relief values from our simulations are shown along the *y*-axis (1 m bins). Sampled age distributions for the sequence boundaries, top clay, and IRSL samples are shown on the *x*-axis (500 year bins). Bivariate age/depth histograms from our simulations are shown with color intensity scaled to probability. Bin widths correspond to the depth and age bins. Trend lines through the mean values are shown, with least squares fitted trend lines for the IRSL data.

Figure 3. Probability normalized histograms of slip rates with 2.5 – 97.5 percentile ranges shown between the stratigraphic boundaries given in the figure titles. Median values are shown for symmetric distributions and modal values for skewed distributions. Bin size is 0.1 mm/yr. The slip-rate similarity plots show the probability of producing fold geometries with similar slip rates from the ages of the boundaries listed in the title across prior intervals, given the uncertainties in our data. The similarity window is the absolute difference in slip rate within which values are considered similar.

[1]GSA Data Repository item 2016xxx, xxxxxxxx, is available online at http://www.geosociety.org/pubs/ft2016.htm or on request from editing@geosociety.org. In addition, seismic reflection data acquired for this study are archived at: https://www.sciencebase.gov/catalog/item/582c9a58e4b04d580bd3786d.

Figure 1

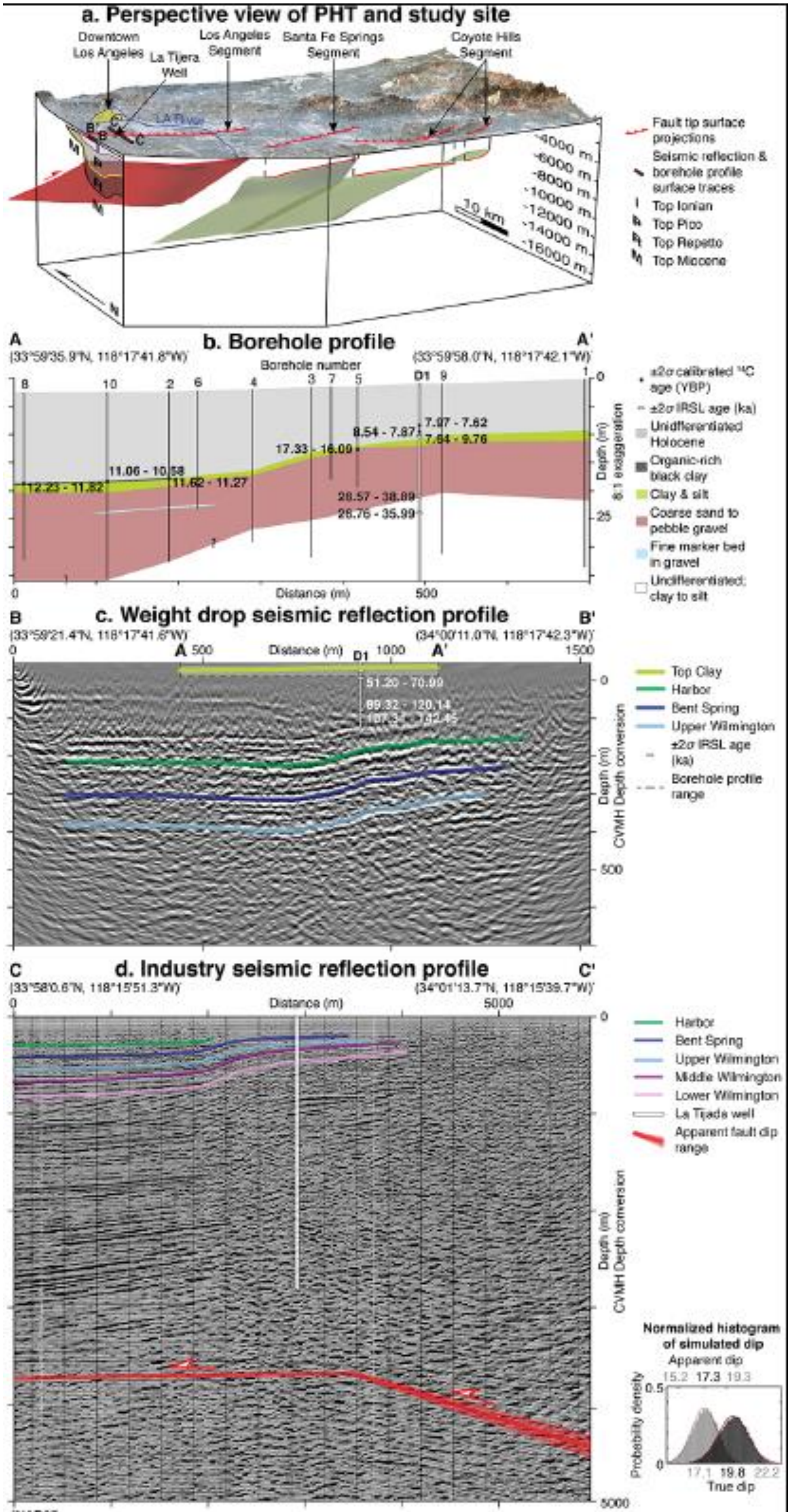
a. Perspective view of PHT and study site
Downtown Los Angeles
La Tijera Well
Los Angeles Segment
Santa Fe Springs Segment
Coyote Hills Segment
LA River
-4000 m
-6000 m
-8000 m
-10000 m
-12000 m
-14000 m
-16000 m
10 km
N
Fault tip surface projections
Seismic reflection & borehole profile surface traces
Top Ionian
Top Pico
Top Repetto
Top Miocene
b. Borehole profile
A
(33°59'35.9"N, 118°17'41.8"W)'
A'
(33°59'58.0"N, 118°17'42.1"W)'
Borehole number
8 10 2 6 4 3 7 5 D1 9 1
12.23 - 11.82
11.06 - 10.58
11.62 - 11.27
17.33 - 16.09
8.54 - 7.87
7.97 - 7.82
7.84 - 9.76
28.57 - 38.89
28.76 - 35.99
Distance (m)
0
500
Depth (m)
8:1 exaggeration
25
±2σ calibrated ¹⁴C age (YBP)
±2σ IRSL age (ka)
Unidifferentiated Holocene
Organic-rich black clay
Clay & silt
Coarse sand to pebble gravel
Fine marker bed in gravel
Undifferentiated; clay to silt
c. Weight drop seismic reflection profile
B
(33°59'21.4"N, 118°17'41.6"W)'
B'
(34°00'11.0"N, 118°17'42.3"W)'
Distance (m)
0 500 1000 1500
D1
51.20 - 70.99
89.32 - 120.14
107.3 - 142.45
Depth (m)
CVMH Depth conversion
500
Top Clay
Harbor
Bent Spring
Upper Wilmington
±2σ IRSL age (ka)
Borehole profile range
d. Industry seismic reflection profile
C
(33°58'0.6"N, 118°15'51.3"W)'
C'
(34°01'13.7"N, 118°15'39.7"W)'
Distance (m)
0
5000
Depth (m)
CVMH Depth conversion
5000
Harbor
Bent Spring
Upper Wilmington
Middle Wilmington
Lower Wilmington
La Tijada well
Apparent fault dip range
Normalized histogram of simulated dip
Apparent dip
15.2 17.3 19.3
Probability density
0.5
0
17.1 19.8 22.2
True dip
'NAD27

Figure 2

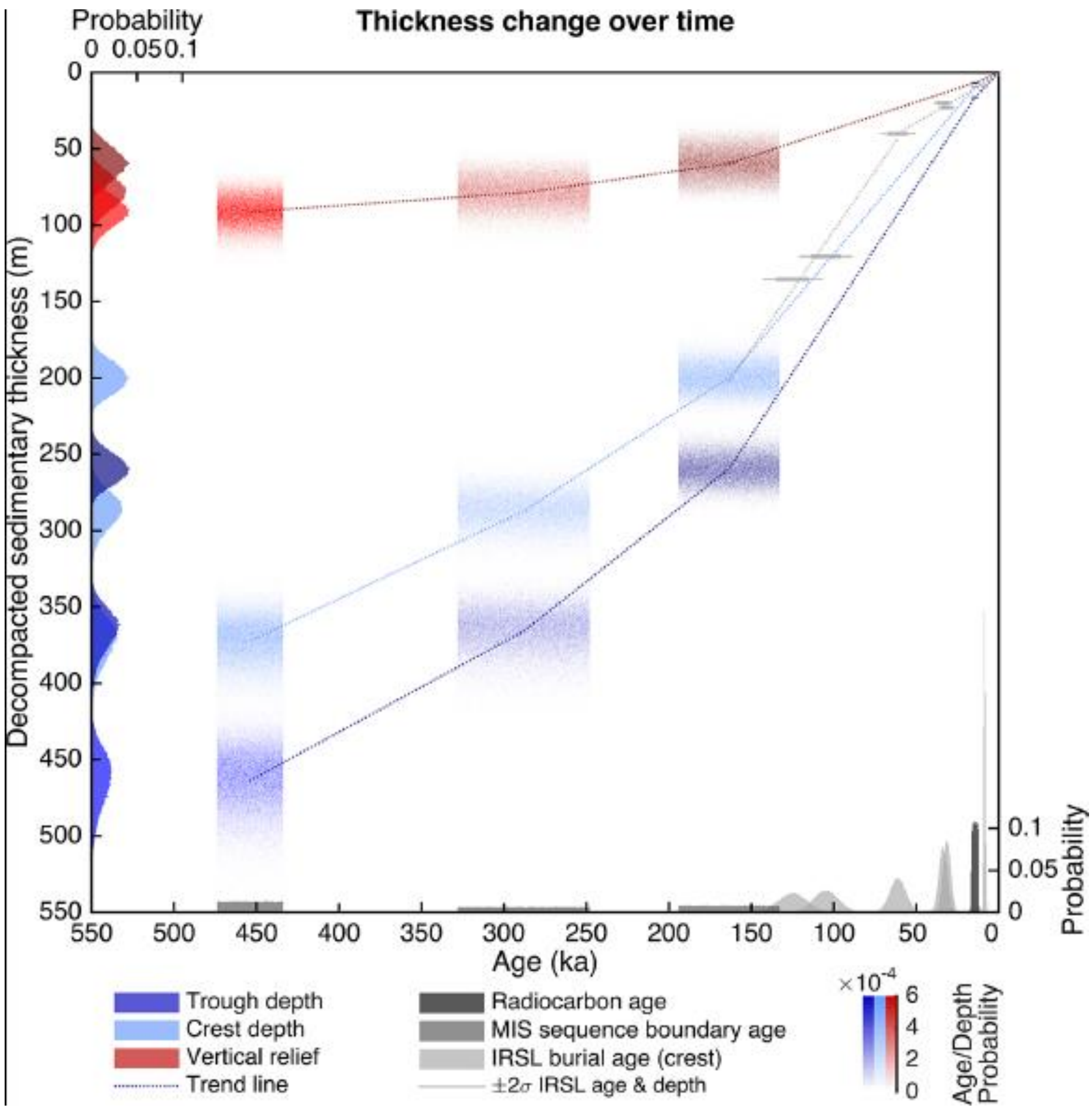
Thickness change over time
Probability
0 0.05 0.1
Decompacted sedimentary thickness (m)
Age (ka)
Probability
0.1
0.05
0
Trough depth
Crest depth
Vertical relief
Trend line
Radiocarbon age
MIS sequence boundary age
IRSL burial age (crest)
±2σ IRSL age & depth
×10⁻⁴
Age/Depth Probability

372 Figure 3

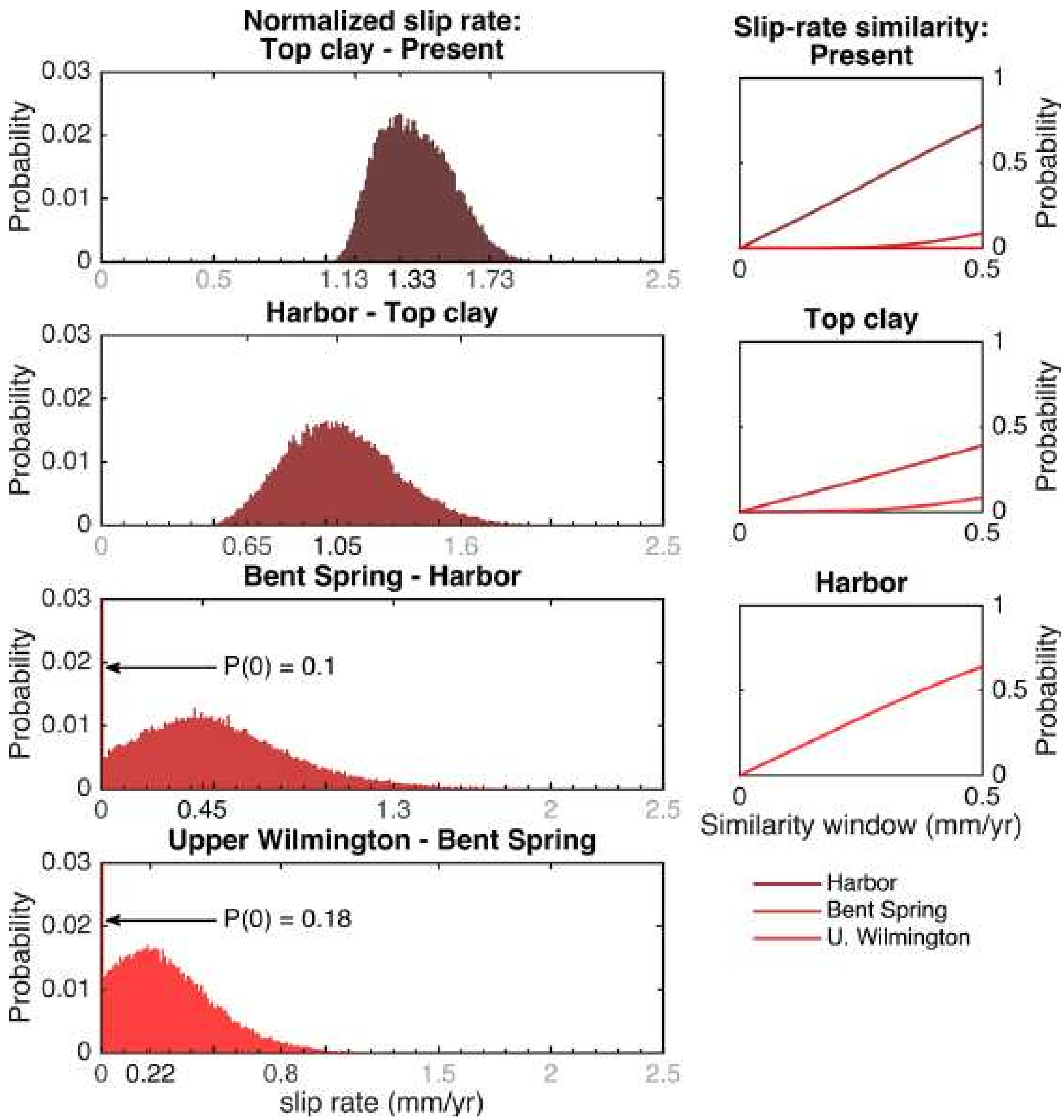
Normalized slip rate:
Top clay - Present
Probability
0.03
0.02
0.01
0
0
0.5
1.13
1.33
1.73
2.5
Harbor - Top clay
0.65
1.05
1.6
Bent Spring - Harbor
P(0) = 0.1
0.45
1.3
2
Upper Wilmington - Bent Spring
P(0) = 0.18
0.22
0.8
1.5
slip rate (mm/yr)
Slip-rate similarity:
Present
Top clay
Harbor
1
0.5
Similarity window (mm/yr)
Harbor
Bent Spring
U. Wilmington